Available online at www.sciencedirect.com

SCIENCE DIRECT®

Talanta 65 (2005) 389–395

Talanta

www.elsevier.com/locate/talanta

Comparison of synchronous and laser-induced fluorescence spectroscopy applied to the Eu(III)-fulvate complexation

K.H. Chung, W. Lee, Y.H. Cho, G.S. Choi, C.W. Lee*

Nuclear Environment Research Division, Korea Atomic Energy Research Institute, 150 Dukjin-Dong, Yuseong-Gu, Daejeon 305-353, South Korea

Received 29 March 2004; received in revised form 7 June 2004; accepted 10 June 2004
Available online 25 August 2004

Abstract

The complexation of europium ion (Eu(III)) with a soil fulvic acid (FA) has been studied at pH 5 in 0.01 M $NaClO_4$ by different experimental methods, i.e. synchronous fluorescence spectroscopy (SyFS) and time resolved laser-induced fluorescence spectroscopy (TRLFS). A series of SyFS quenching spectra was obtained by increasing the Eu(III) concentration and keeping the FA concentration constant. The emission spectra and fluorescence lifetimes of the Eu(III) bound to the FA were also measured by a TRLFS system using the same solution used in the SyFS spectral measurement. From the analysis of the fluorescence data obtained by the SyFS and the TRLFS using a non-linear least-squares method, the concentration of the binding sites (C_L) of the FA accessible for the Eu(III) and the corresponding conditional stability constants ($\log K$) were estimated. The two different methods gave rise to constants being comparable with one another. The $\log K$ and C_L values (mean ± standard deviation of three determinations) determined by the SyFS were 6.4 ± 0.2 ($6.7 \pm 0.1\ \mu mol\ L^{-1}$: by the TRLFS) and $10 \pm 1\ \mu mol\ L^{-1}$ ($7 \pm 1\ \mu mol\ L^{-1}$: by the TRLFS), respectively. The applicability of the FA fluorescence quenching techniques for estimating the europium binding parameters was proved by the direct monitoring of the Eu(III) bound to the FA using the TRLFS system.

Keywords: Fulvic acid; Synchronous fluorescence; TRLFS; Eu(III)-fulvate complexation; Stability constant

---

1. Introduction

Humic substances (HS), namely humic acid (HA) and fulvic acid (FA), are naturally occurring organic matters which have a high affinity to metal ions, and strongly influence the speciation of metal ions in a terrestrial and aquifer system [1–3]. The determination of the complexing properties of HS with metal ions is not only important from the ecotoxicological viewpoint, but also it is required for the understanding of metal ions transport and speciation in terrestrial and aquatic environments.

The humate and fulvate complexation behavior of metal ions have been studied by a number of investigators with a variety of analytical methods [4–13]. These include electrochemical method [4], solvent extraction [5,6], ion exchange [7], equilibrium dialysis [8,9], ultrafiltration [10] and spectroscopic methods [11–14]. Most of these techniques measure unbound metal ions or both unbound and bound metal ions simultaneously. While the fluorescence quenching method, which is based on the quenching of ligand fluorescence caused by addition of metal ion, measures unbound ligand [4,15–24]. It was introduced in the early 1980s as an alternative for the analysis of complexes between HS and metal ions [4,15]. Emission and synchronous fluorescence methods have been used in the past to establish the extent of metal ion binding to HS. Synchronous fluorescence spectra, as compared with emission spectra, give more information on the distribution of fluorephores in HS [17–24]. Recently, a self-modeling mixture analysis technique has been used to analyze synchronous fluorescence spectroscopy (SyFS) spectral data and to further detect the wavelength where the strongest quenching occurs [25–27]. Although the fluorescence quenching spectroscopy remains popular as a tool for measuring the extent of metal ion binding by HS, its validity has been questioned [18,20]. The key assumption that the

---

* Corresponding author. Tel.: +82 42 868 2296; fax: +82 42 8631289.
E-mail address: cwlee@kaeri.re.kr (C.W. Lee).

0039-9140/$ – see front matter © 2004 Elsevier B.V. All rights reserved.
doi:10.1016/j.talanta.2004.06.026

remaining quenchable fluorescence uniformly measures the remaining free ligand concentration has led to a debate in the literature [21,22]. Recently, the validity of the fluorescence quenching techniques was tested by the TRLFS measurements [23]. However, it was not a direct comparison between the two methods: different experimental conditions were used in each method. In the SyFS measurements, the europium ion (Eu(III)) concentration was varied and the HA concentration was kept constant. While the time resolved laser-induced fluorescence spectroscopy (TRLFS) measurements were conducted by increasing the HA concentration and keeping the Eu(III) concentration constant. It is reported that the stability constant seems to be affected by the cation concentration, pH and ionic strength [8,12,13].

In this study, the complexation of Eu(III) with the FA is described. The metal ion Eu(III) is selected because it has good fluorescence properties and represents a good chemical analogue for the actinide metals which constitute a radiological hazard [8,11,12,25]. The FA, the most soluble fraction of HS, is one of the constituents of soil organic matter; and therefore, it is thought to have a special role in the environmental mobility of metal ions [28]. Synchronous fluorescence is used because it gives a higher resolution spectrum and may allow to measure the corresponding fluorescent fractions of the FA accessible for the Eu(III) [17,20,25].

The objectives of this study were to investigate the binding of Eu(III) to the FA using a SyFS and a TRLFS system and to compare the results obtained by the two different experimental methods. The TRLFS system, which can directly monitor unbound and bound Eu(III) to the FA, was used to test the applicability of the FA fluorescence quenching technique for estimating the europium binding parameters.

2. Experimental

2.1. Humic substances

The HS used in this study was isolated from soil sampled at the Jeju Island in Korea. Detailed information for the sites has been described elsewhere [29]. The HS was extracted and further purified by the procedures of IHSS [30]. After extraction and purification of HS, the protonated final humic and fulvic aicds were freeze-dried and kept in a vacuum desiccator.

2.2. Synchronous fluorescence spectroscopy

Stock solutions of the FA and Eu(III) ion were 100 mg L^{-1} and 2.0×10^{-4} mol L^{-1} at pH 5.0 in 0.01 M $NaClO_4$, respectively. A series of samples was prepared by mixing the appropriate quantities of the two stock solutions and 0.01 M $NaClO_4$. The Eu(III) concentrations were varied from 1.0×10^{-6} to 2.8×10^{-5} mol L^{-1} in 20 different concentrations and the FA concentration was kept constant at 10.0 mg L^{-1}.

The solutions were shaken for ca. 2 min and the pH was adjusted to 5.0 ± 0.1 with NaOH and $HClO_4$. Spectroscopic measurements were taken immediately following the sample preparation. The SyFS spectral measurements were made with the luminescence spectrometer AB 2 (AMINCO-Bowman). For these measurements, slit widths were set at 4 and 8 nm for the excitation and emission monochromators, respectively. The SyFS spectra were recorded for the samples at an emission wavelength ranging 250–650 nm and at a scan rate of 4 nm s^{-1}. The wavelength difference ($\Delta\lambda$) was 30 nm between the excitation and emission monochromators. The effect of varing $\Delta\lambda$ on the shape of SyFS spectra was investigated in our preliminary study and a value of $\Delta\lambda = 30$ nm resulted in the best overall spectral resolution [27].

2.3. Time resolved laser-induced fluorescence spectroscopy

The emission spectra and fluorescence lifetimes of Eu(III) bound to the FA were also measured by a TRLFS system using the same solution used in the SyFS spectral measurements. A pulsed Nd-YAG laser (YAG5011 COMP10, B.M. industries) operating at 355 nm (third harmonic output) and delivering about 5 mJ energy in a 5 ns pulse width with a repetition rate of 10 Hz was used to excite the europium ion. The emitted fluorescence light was focussed into a spectrograph (HR 320, Jobin Yvon; with 600 g mm^{-1} grating) at a right angle to the excitation laser beam. The spectrograph was centered at 590 nm and in a dispersion of the spectral range 540–650 nm to observe the direct line fluorescence of europium. The intensified CCD-detector (iStar, ENDOR Technology) was used for the detection of the fluorescence signal. An external trigger from the Nd-YAG laser activates the digital delay generator built into the ICCD, so that the digital delay generator can control the intensifier tube for gating application. Time resolved experiments were performed using a delay time of 15 μs with respect to the initial laser pulse, a gate time step of 15 μs and a gate width for fluorescence of 1500 μs.

3. Results and discussion

3.1. Complexation study by SyFS

The fluorescence quenching of the FA by an addition of the Eu(III) was measured at the FA concentration of 10 mg L^{-1}, with the Eu(III) ranging 1.0×10^{-6} to 2.8×10^{-5} mol L^{-1}. The SyFS spectra for a series of samples are illustrated in Fig. 1. These spectra showed four distinct peaks at 320, 392, 420 and 498 nm. The peak at 320 nm could be due to the Raman emission of the solvent water, which appeared in the blank solution [17]. When water of high purity (fluorescence-free) was excited at 290 nm, the Raman band of water in the emission spectrum was observed at a wavelength of 320 nm. The second and forth peaks were relatively sharp but the third peak centered at about 420 nm was broad. The three major peaks are attributed to the different fluorophores of the FA. The fluorescence properties of the various fluorophores of

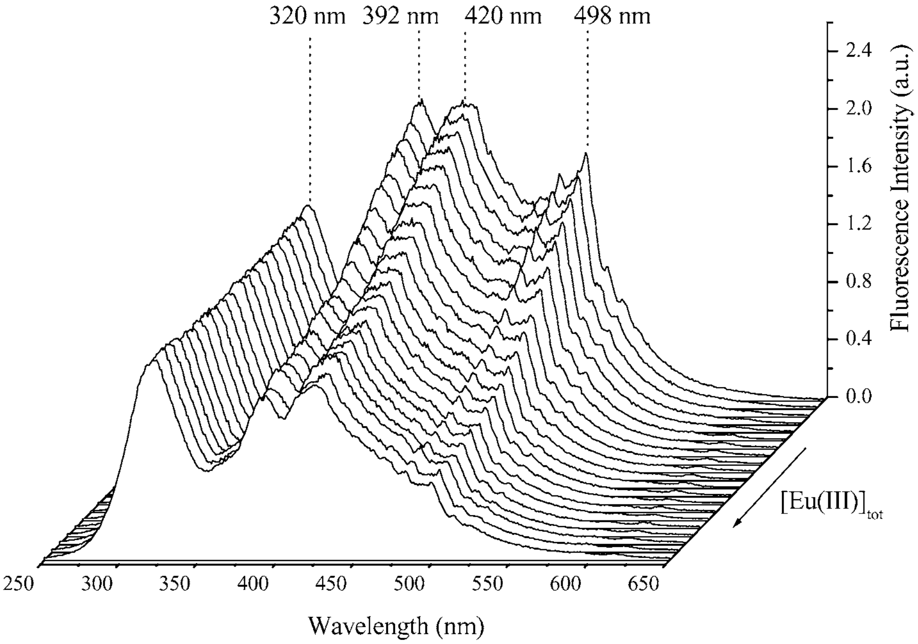

Fig. 1. The SyFS quenching spectra of FA as a function of the Eu(III) concentration: pH 5; [Eu(III)] = 1.0×10^{-6} to 2.8×10^{-5} mol L^{-1}; and [FA] = 10.0 mg L^{-1}.

the HS are well discussed elsewhere [17,27,31]. All of these three distinct peaks showed a decrease in the fluorescence intensity by a quenching of the Eu(III) as its concentration was increased. However, the strongest relative quenching was observed at 498 nm among the three major peaks. So, the quenching profile at 498 nm was further analyzed to estimate the conditional stability constant and the binding site concentration. In Fig. 2, the relative fluorescence intensity at 498 nm is plotted against the total europium concentration.

The concentration of the binding sites of FA accessible to the Eu(III) and the corresponding conditional stability constants can be estimated by the analysis of the quenching profile (Fig. 2) using non-linear least-squares method with the equation below [15,16,27].

$$I = \frac{I_{\mathrm{ML}} - 100}{2KC_{\mathrm{L}}}\{(KC_{\mathrm{L}} + KC_{\mathrm{M}} + 1) - [(KC_{\mathrm{L}} + KC_{\mathrm{M}} + 1)^2 - 4K^2C_{\mathrm{L}}C_{\mathrm{M}}]^{1/2}\} + 100 \qquad (1)$$

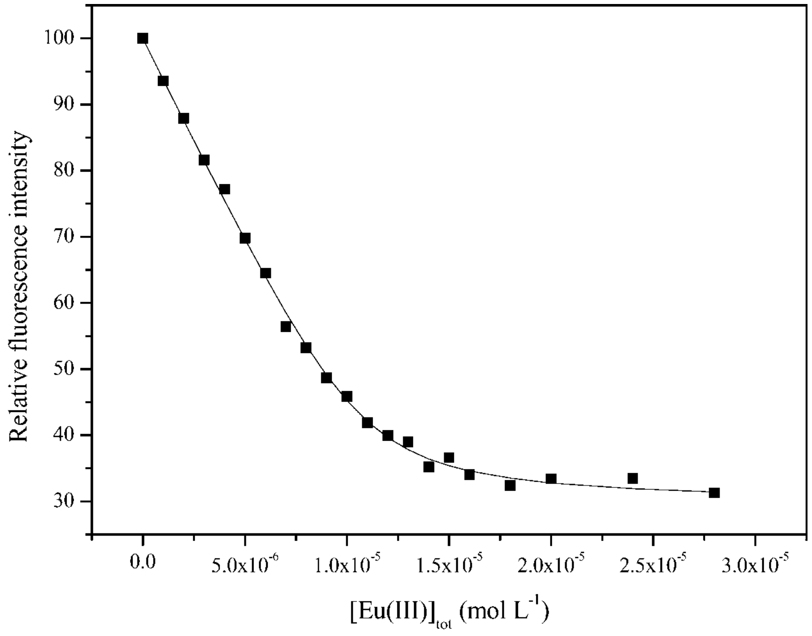

Fig. 2. Fluorescence quenching profiles of FA at 498 nm. Experimental data are shown as solid squares and the solid line indicates the fitted result.

Table 1
Equilibrium parameters obtained by the SyFS and TRLFS[a]

	SyFS	TRLFS	
		$F_{592,0}$	$F_{616,0}$
$\log K$	6.4 ± 0.2	6.7 ± 0.1	6.7 ± 0.2
C_L	10 ± 1	7 ± 1	6 ± 1
I_{ML}	30 ± 2	–	–
$\alpha_{616}/\alpha_{592}$	–	1.0	2.8 ± 0.4

[a] $\log K$: logarithm of the conditional stability constants (mol^{-1} L); C_L: concentration of the ligand (μmol L^{-1}); I_{ML}: limiting fluorescence intensity at maximum metal–ligand binding condition; α_{592} and α_{616}: proportional constants at 592 and 616 nm. The values of $\log K$, C_L and I_{ML} are listed as mean ± standard deviation of three independent experiments.

Table 2
Spectroscopic properties of the Eu(III) species[a]

$[\mathrm{FA}]_{\mathrm{tot}}$	$[\mathrm{Eu(III)}]_{\mathrm{tot}}$	F_{rel} (592 nm)	F_{rel} (616 nm)
0	20	1	1
10	20	260	410
10	1	40	95

[a] $[\mathrm{FA}]_{\mathrm{tot}}$: total concentration of the FA (mg L^{-1}); $[\mathrm{Eu(III)}]_{\mathrm{tot}}$: total concentration of the Eu(III) ion (μmol L^{-1}); F_{rel} (592 nm) and F_{rel} (616 nm): relative fluorescence intensities at 592 and 616 nm.

where I is the fluorescence intensity, K is the conditional stability constant, C_L and C_M are the total FA and Eu(III) concentrations and I_{ML} is the limiting fluorescence intensity at maximum metal–ligand binding condition. Using the experimental data (I and C_M), this equation can be solved for K, C_L and I_{ML}. The optimized equilibrium parameters are listed in Table 1. The results indicate that the conditional stability constant ($\log K$) is 6.4 ± 0.2 mol^{-1} L and the total site concentration (C_L) of 10.0 mg L^{-1} of the FA is 10 ± 1 μmol L^{-1}. The estimated C_L value of the FA used in this work is lower than the one (22.1 μmol L^{-1}) observed for the soil fulvic acid (10 mg L^{-1}) with the Cu(II) ion at pH 5 [15]. This may be due to low amount of proton exchange sites of the FA used in this study [32]. The residual fluorescence (I_{ML}) value can be experimentally determined to be about 30 in Fig. 2. However, the I_{ML} value could also be fitted very well with K and C_L in this study. The optimized I_{ML} value by the fitting was in good agreement with the experimentally determined value.

3.2. Complexation study by TRLFS

When a non-complexed Eu(III) ion is excited by using a pulsed Nd-YAG laser operating at 355 nm, two main fluorescence peaks are observed at 592 nm (magnetic dipole $^5D_0$–$^7F_1$ transition) and 616 nm (hypersensitive $^5D_0$–$^7F_2$ transition). Two peaks were also observed at the same positions by an excitation of a non-complexed Eu(III) ion at 308 or 394 nm [11,12,23]. When the Eu(III) is complexed with the FA, the two main peak positions do not change but the intensity of the peaks is increased (Fig. 3). In addition, a weak band is observed at 580 nm (non-degenerated $^5D_0$–$^7F_0$ transition). In general, the fluorescence spectrum of the non-complexed Eu(III) ion exhibits the most intensive peak at 592 nm. However, the hypersensitive $^5D_0$–$^7F_2$ transition peak (616 nm) becomes the most intense as the Eu(III) is bound to the FA.

Fig. 3 shows the fluorescence spectra of the non-complexed Eu(III) ion and the Eu(III) bound with the FA. The spectroscopic properties of the Eu(III) are summarized in Table 2. Upon the complexation of the Eu(III) of 20 μmol L^{-1} to the FA of 10.0 mg L^{-1}, the total intensities

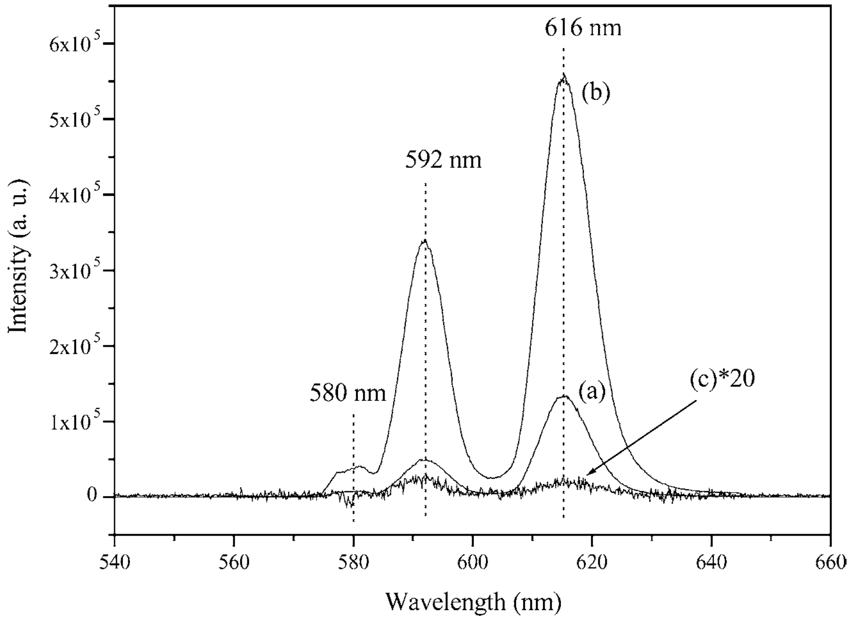

Fig. 3. Fluorescence spectra of the Eu(III) in the absence and presence of the FA: (a) [Eu(III)] = 1 μmol L^{-1}, [FA] = 10 mg L^{-1}; (b) [Eu(III)] = 20 μmol L^{-1}, [FA] = 10 mg L^{-1}; and (c) [Eu(III)] = 20 μmol L^{-1}, [FA] = 0 mg L^{-1}. The spectrum of (c) is scaled by 20.

of the fluorescence peaks at 592 and 616 nm are dramatically enhanced by a factor of 260 and 410 relative to the non-complexed Eu(III) ion, respectively. This is due to the sensitized Eu(III) luminescence following the intramolecular energy transfer from the FA to Eu(III) excited levels [33]. The intensity at 616 nm was much more enhanced due to the hypersensitive $^5D_0$–$^7F_2$ transition of the Eu(III) bound to the FA [11,12,23]. These properties of the sensitized luminescence and hypersensitive transition of the Eu(III) are very important for the complexation study. The measured fluorescence intensities are mainly caused by the Eu(III) bound to the FA. The excitation of the non-complexed Eu(III) ion has hardly any contribution to the measured fluorescence in this experimental condition where the non-complexed Eu(III) ions are presented with less than 20 μmol L^{-1} (see Table 2). Therefore, the fluorescence intensities (F_i) at 592 and 616 nm, considering that the ligand exchange reaction does not take place within the excited state lifetime [34], are directly proportional to the Eu(III) bound to the FA. The relationship between the fluorescence intensity (F_i) and the concentration of the Eu(III) bound to the FA can be expressed as:

$$F_i = \alpha_i[\mathrm{ML}] \quad (2)$$

where the α_i values are the proportional constants (i= 592 and 616 nm) and dependent on the instrument setup as well as the sample characteristics. This equation is similar to the ones used to calculate the stability constants of the Eu(III) bound to the HS with the TRLFS measurements by increasing the HS concentration and keeping the Eu(III) concentration constant [12,23].

Based on the mass balances between Eu(III) and FA (1:1 stoichiometry), the concentration of Eu(III) bound to the FA ([ML]) can be written in terms of the conditional stability constant (K), total Eu(III) concentration (C_M) and total FA concentration (C_L):

$$[\mathrm{ML}] = \frac{1}{2K}\{(KC_\mathrm{L} + KC_\mathrm{M} + 1) - [(KC_\mathrm{L} + KC_\mathrm{M} + 1)^2 - 4K^2C_\mathrm{L}C_\mathrm{M}]^{1/2}\} \quad (3)$$

A combination of Eqs. (2) and (3) gives the relationship between the fluorescence intensity (F_i) and the total metal ion concentration (C_M):

$$F_i = \frac{\alpha_i}{2K}\{(KC_\mathrm{L} + KC_\mathrm{M} + 1) - [(KC_\mathrm{L} + KC_\mathrm{M} + 1)^2 - 4K^2C_\mathrm{L}C_\mathrm{M}]^{1/2}\} \quad (4)$$

Using the experimental data (F_i and C_M), this equation can be solved for K, C_L and α_i.

The fluorescence intensity ($F_{i,0}$) at t = 0 can be obtained from the analysis of the time dependent fluorescence spectra shown in the Fig. 4. The fluorescence intensities at 592 and 616 nm are integrated from 583 to 603 nm and from 603 to 643 nm, respectively. The relaxation of fluorescence emission at 592 nm for the selected samples is shown in Fig. 5. The natural logarithm of the intensity at 592 nm is plotted as a function of the delay. A non-monoexponential decay pattern is observed at all the europium concentration ranges. At low values of the total europium concentration (Fig. 5 (a)), a slow decay component (τ_1) is predominant. However, a fast decay component (τ_2) becomes dominant as the Eu(III) concentration is increased (Fig. 5 (f)). The multi-exponential decay does not correspond to the different binding sites but is ascribed to the quenching process [34]. The time dependency of the fluorescence intensity can be analyzed by a bi-exponential function:

$$F_{i,t} = F_{i,0}[x\exp(-t/\tau_1) + (1-x)\exp(-t/\tau_2)] \quad (5)$$

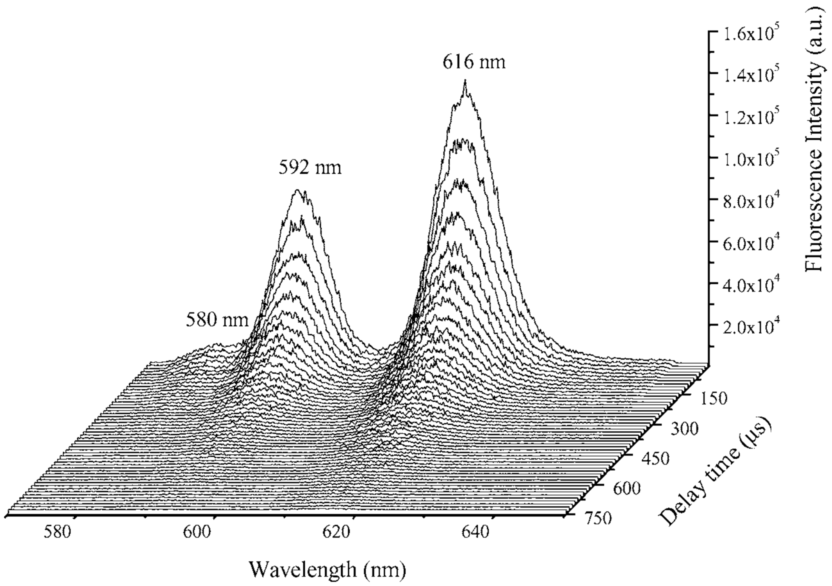

Fig. 4. Fluorescence spectra of the Eu(III) bound to the FA at different gate pulse delay time: pH 5; [Eu(III)] = 20 μmol L^{-1}; and [FA] = 10.0 mg L^{-1}.

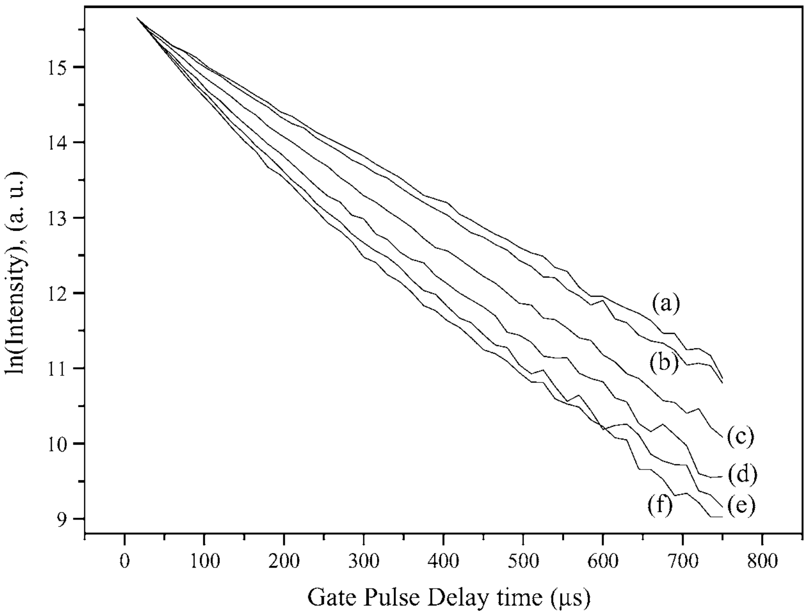

Fig. 5. Time dependency of the fluorescence emission of the Eu(III) bound to the FA of 10 mg L^{-1} at various Eu(III) concentrations: (a) [Eu(III)] = 2 μmol L^{-1}; (b) [Eu(III)] = 4 μmol L^{-1}; (c) [Eu(III)] = 8 μmol L^{-1}; (d) [Eu(III)] = 12 μmol L^{-1}; (e) [Eu(III)] = 16 μmol L^{-1}; and (f) [Eu(III)] = 20 μmol L^{-1}. The decay curves ((a)–(e)) are scaled to the same total emission of the (f) at t = 15 μs.

where t is the gate pulse delay time, $F_{i,t}$ and $F_{i,0}$ are the fluorescence intensity at $t = t$ and 0 (i = 592 and 616 nm), respectively, τ_1 and τ_2 are the lifetimes of the two components and x is the fraction of the first component contributed to the total fluorescence intensity. Using the experimental data ($F_{i,t}$, t), the fluorescence intensity ($F_{i,0}$) at t = 0 was estimated by Eq. (5) where τ_1 is fixed at 155 μs. The lifetime (τ_1) of the slow component was reasonably calculated to be 155 ± 3 μs by a monoexponential decay pattern using the curve obtained with the low values of the total europium concentration (Fig. 5 (a)). The lifetime (τ_2) of the fast component was estimated to be 74 ± 5 μs. This value is shorter than the fluorescence lifetime of the non-complexed Eu(III) ion (110 μs), which was obtained at the Eu(III)

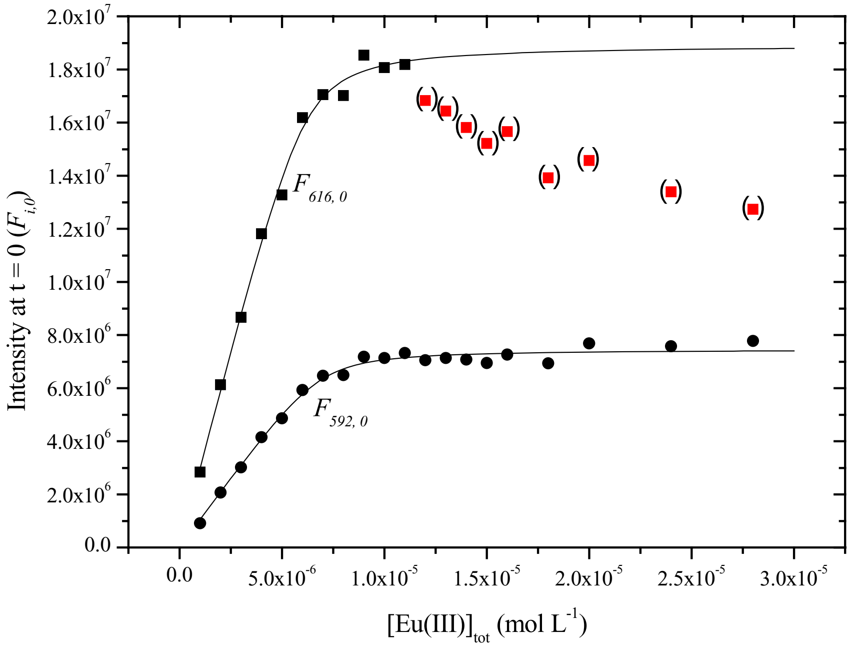

Fig. 6. Change of the fluorescence intensity of the Eu(III) bound to the FA as a function of the Eu(III) concentration: pH 5, [Eu(III)] = 1.0×10^{-6} to 2.8×10^{-5} mol L^{-1}, [FA] = 10.0 mg L^{-1}. Experimental data are shown as symbols, and the solid lines indicate the fitted results. The data deviated from the plateau (in brackets) at $F_{616,0}$ were not included to fit the data.

concentration of 2×10^{-2} mol L^{-1}. Fig. 6 shows the change of the fluorescence intensities ($F_{i,0}$) attributed to the Eu(III) bound to the FA as a function of the Eu(III) concentration. The intensity at 616 nm is steadily decreased after the plateau region, which is not expected by Eq. (2). This observation may be due to self-quenching effect at high concentration of Eu(III). Further work is needed to elucidate this problem.

From the analysis of the TRLFS spectral data shown in Fig. 6 using Eq. (5), the equilibrium parameters were optimized and listed in Table 1. The results indicate that the $\log K$ and C_L values estimated from the $F_{592,0}$ are 6.7 ± 0.1 mol^{-1} L (6.7 ± 0.2 mol^{-1} L from the $F_{616,0}$) and 7 ± 1 μmol L^{-1} (6 ± 1 μmol L^{-1} from the $F_{616,0}$), respectively. These values are comparable with the ones obtained by the SyFS method described above. The proportional constant (α_{616}) for the peak at 616 nm was three times higher than the value of α_{592}. This can be explained by the proportionality of the α_i values to the maximum fluorescence intensity.

4. Concluding remarks

The two different experimental methods provided comparable values for the conditional stability constants. The $\log K$ values determined by the SyFS and TRLFS were 6.4 ± 0.2 and 6.7 ± 0.1 mol^{-1} L, respectively. The data of this study are in good agreement with other published results: $\log K = 6.83 \pm 0.99$ (pH 2.7–6.5; $I = 0.1$ M) and 6.30 ± 0.36 (pH 2.7–6.5; $I = 1.0$ M) [12]. The values for Eu(III) reported in Table 1 are close to the conditional stability constants for the actinides (Am^{3+} and Cm^{3+}) complexation of the HS obtained from various experimental methods [32]. The applicability of the FA fluorescence quenching technique for estimating the europium binding parameters was proved by the direct monitoring of the Eu(III) bound to the FA using the TRLFS system. The ligand fluorescence quenching technique may be effectively used for the complexation study between the HS and the paramagnetic metal ions with a low fluorescence yield.

Acknowledgement

This study has been carried out under the nuclear R&D program by the Ministry of Science and Technology (MOST) of Korea.

References

[1] J. Buffle, Complexation Reactions in Aquatic Systems, Ellis Horwood Limited, New York, 1988 (p. 16).
[2] J.I. Kim, Chemical behaviour of transuranic elements in natural aquatic systems, in: A.J. Freeman, C. Keller (Eds.), Handbook on the physics and Chemistry of the Actinides, North Holland, Amsterdam, 1986, p. 413.
[3] F.J. Stevenson, Geochemistry of soil humic substances, in: G.R. Aiken, D.M. McKnight, R.L. Wershaw, P. MacCarthy (Eds.), Humic Substances in Soil, Sediment and Water, Wiley, New York, 1985, p. 13.
[4] R.A. Saar, J.H. Weber, Anal. Chem. 52 (1980) 2905.
[5] R.A. Torres, G.R. Choppin, Radiochim. Acta 35 (1984) 143.
[6] Y. Takahashi, Y. Minai, Y. Meguro, S. Toyoda, J. Radioanal. Nucl. Chem. Lett. 186 (1994) 129.
[7] A. Maes, J. De Brabandere, A. Cremers, Radiochim. Acta 44/45 (1988) 51.
[8] J.R. Lead, J. Hamilton-Taylor, A. Peters, S. Reiner, E. Tipping, Anal. Chim. Acta 369 (1998) 171.
[9] M.A. Glaus, W. Hummel, L.R. Van Loon, Appl. Geochem. 15 (2000) 956.
[10] M.S. Caceci, Radiochim. Acta 39 (1985) 51.
[11] J.C. Dobbs, W. Susetyo, F.E. Knight, M.A. Castles, L.A. Carreira, L.V. Azarraga, Anal. Chem. 61 (1989) 483.
[12] G. Bidoglio, I. Grenthe, P. Qi, P. Robouch, N. Omennetto, Talanta 38 (1991) 999.
[13] V. Moulin, J. Tits, C. Moulin, P. Decambox, P. Mauchien, O. De Ruty, Radiochim. Acta 58/59 (1992) 121.
[14] J.I. Kim, D.S. Rhee, H. Wimmer, G. Buckau, R. Klenze, Radiochim. Acta 62 (1993) 35.
[15] D.K. Ryan, J.H. Weber, Anal. Chem. 54 (1982) 986.
[16] C.-F. Lin, D.-Y. Lee, W.-T. Chen, K.S. Lo, Environ. Pollut. 87 (1995) 181.
[17] N. Senesi, Anal. Chim. Acta 232 (1990) 77.
[18] S.E. Cabaniss, M.S. Shuman, Anal Chem. 60 (1988) 2418.
[19] S.E. Cabaniss, Environ. Sci. Technol. 26 (1992) 1133.
[20] R.L. Cook, C.H. Langford, Anal. Chem. 67 (1995) 174.
[21] D.K. Ryan, L.S. Ventry, Anal. Chem. 62 (1990) 1523.
[22] S.E. Cabaniss, M.S. Shuman, Anal. Chem. 62 (1990) 1526.
[23] G. Bidoglio, D. Ferrari, E. Selli, F. Sena, G. Tamborini, Environ. Sci. Technol. 31 (1997) 3536.
[24] X. Lu, R. Jaffe, Water Res. 35 (2001) 1793.
[25] J.C.G. Esteves da Silva, A.A.S.C. Machado, C.J.S. Oliveira, Analyst 121 (1996) 1373.
[26] J.C.G. Esteves da Silva, A.A.S.C. Machado, C.J.S. Oliveira, M.S.S.D.S. Pinto, Talanta 45 (1998) 1155.
[27] H.S. Shin, K.H. Hong, M.H. Lee, Y.H. Cho, C.W. Lee, Talanta 53 (2001) 791.
[28] J.H. Weber, Binding and transport of metals by humic materials, in: F.H. Frimmel, R.F. Christman (Eds.), Humic Substances and Their Role in the Environment, Wiley, New York, 1988, p. 165.
[29] M.H. Lee, C.W. Lee, J. Radioanal. Nucl. Chem. 239 (1999) 471.
[30] IHSS: Isolation of IHSS soil fulvic and humic acids, in: International Humic Substances Society, http://www.ihss.gatech.edu/.
[31] T.M. Miano, N. Senesi, Sci. Total Environ. 117/118 (1992) 41.
[32] K.R. Czerwinski, J.I. Kim, D.S. Rhee, G. Buckau, Radiochim. Acta 72 (1996) 179.
[33] C.-D. Tiseanu, M.U. Kumke, F.H. Frimmel, R. Klenze, J.I. Kim, J. Photochem. Photobiol A: Chem. 117 (1998) 175.
[34] P. Panak, R. Klenze, J.I. Kim, H. Wimmer, J. Alloys Compd. 225 (1995) 261.